

Some Gross Features of Single-Particle Spectra at Energies above 10^4 GeV and Comparisons with Data at 28.5 GeV

L. von Lindern

Brookhaven National Laboratory, Upton, New York 11973†*

and

R. S. Panvini

Brookhaven National Laboratory, Upton, New York 11973, and
Vanderbilt University, Nashville, Tennessee 37203‡*

and

J. Hanlon and E. O. Salant

Vanderbilt University, Nashville, Tennessee 37203‡
(Received 6 October 1971)

Single-particle spectra from multiparticle production in pp collisions at 28.5 GeV/ c from bubble-chamber data are compared with cosmic-ray emulsion data above 10^4 GeV. The spectrum at high energies does not develop a plateau as expected from multiperipheral models, and the target-fragmentation cross section decreases, approximately as $1/\ln s$.

Much attention has been given recently to predictions that hadronic multiparticle spectra of high-energy particle collisions approach finite energy-independent limits.¹ Tests have come mainly from experiments below 30 GeV,^{2,3} from the cosmic-ray experiment of Jones *et al.*,⁴ and from the CERN intersecting storage rings⁵ at primary energies corresponding to laboratory energies $\sim 10^3$ GeV. In this Letter, another order of magnitude is gained by comparing 28-GeV pp collisions in a bubble chamber with cosmic-ray interactions at $\approx 10^4$ GeV in nuclear emulsions.

We study single-particle inclusive distributions; i.e.,

$$a + b \rightarrow c + \text{anything}, \quad (1)$$

where a is the beam particle, b the target, and c any charged secondary particle whose distribution we plot. A single event contributes as many entries to a plot as it has charged prongs c . The total inclusive cross section for charged secondary particles then is

$$\Sigma_I \equiv \bar{n}_s \sigma_{\text{tot}}, \quad (2)$$

where \bar{n}_s is the mean multiplicity of charged secondaries and σ_{tot} is the total cross section of included events.

In cosmic-ray emulsions, track angles are measured. Because of its unique Lorentz-transformation properties, the variable U_L is chosen, where

$$U_L = \log_{10} \tan \theta_L, \quad \theta_L < 90^\circ, \quad (3)$$

L denoting lab quantities and θ the polar angle with respect to the incident particle direction. U_L is a good approximation to the rapidity⁶ y which satisfies the Lorentz-invariant condition $dy = dp_{\parallel}/E$ and

$$y \equiv \frac{1}{2} \log_{10} \left(\frac{E + p_{\parallel}}{E - p_{\parallel}} \right) = -\log \left[\frac{(p_{\perp}^2 + m^2)^{1/2}}{E + p_{\parallel}} \right] \quad (4)$$

in any rest frame, where p_{\perp} and p_{\parallel} are incident momentum components, and m and E are the mass and energy of particle c . From (4), it follows that

$$y_L = y_C + \log_{10} [\gamma(1 + \beta)] \xrightarrow{\gamma \gg 1} y_C + \log_{10}(2\gamma), \quad (5)$$

with $\gamma = (1 - \beta^2)^{-1/2}$ the Lorentz factor for lab to c.m. (C) transformations, showing that shapes of distributions in y (or, to a good approximation, U_L) are the same in different frames, and only the scale is shifted.

At these cosmic-ray energies the variable U_L is closely related to y_L and therefore to y_C . Secondary particles in these collisions are mainly pions, with mean transverse momentum $\bar{p}_{\perp} \sim 0.4$ GeV/ c . It follows that $p_{\parallel,L}^2 \gg p_{\perp}^2 \gg m_{\pi}^2$ for most secondaries, so that

$$-U_L \rightarrow y_C + \log_{10} \gamma \quad (6)$$

from (3), (4), and (5). The distribution of charged secondaries in a typical high-energy event is approximately symmetric in the c.m. system, so that the mean value $\bar{y}_C = 0$. Therefore the mean value $\bar{U}_L = \log_{10} \gamma$ is a measure of the primary energy (Castagnoli technique), i.e., $E_{\text{prim}} \approx 2\gamma^2 \times (\text{tar}$

get mass).

Before discussing comparisons, some facts about the data are outlined:

(1) Hydrogen-like events in photographic emulsions are chosen by accepting only events with a small number (N_h) of accompanying heavily ionizing prongs. When $N_h \lesssim 5$, it has been shown that mean multiplicities and angular distributions are very similar to pure hydrogen events, whereas for much larger values of N_h significant differences occur.⁷

(2) The primary energy of the cosmic-ray events at $\approx 10^4$ GeV was determined by the Castagnoli method,⁸ which has been established near 30 GeV with accelerator beams of known energy.⁹ If highly asymmetric events (backward in the c.m. system) escape classification because of an underestimate of the Castagnoli energy, their forward asymmetric counterparts should be seen (in forty events only one such candidate was found).

(3) Spectra of cosmic-ray secondaries are plotted only for tracks with ionization < 1.4 of the minimum in order to reject nuclear evaporation prongs. For consistency, the bubble-chamber tracks plotted have a velocity $\beta > 0.7$ to correspond to the ionization cut in the cosmic-ray data.

(4) The cosmic-ray sample consists of forty interactions with neutral as well as singly charged primaries (protons and pions) from the University of Chicago group¹⁰ and ICF collaboration¹¹ (both sets were scanned with similar criteria). The Castagnoli method yields 34 events with primary energies 10^4 – 10^5 GeV and 6 events with more than 10^5 GeV. The observed mean multiplicity \bar{n}_s is 18.8, and $\bar{N}_h = 3$. Only events with $n_s \geq 7$ are chosen because of larger scanning losses¹² for lower multiplicities; however, the expected number of events with $n_s \leq 6$ is negligible at $\geq 10^4$ GeV. Accounting for the missing events we estimate that the "true" mean multiplicity is not smaller than 15. This value also allows for a slight increase in multiplicity caused by interactions of secondaries within the nucleus.

(5) To check the validity of the cosmic-ray analyses, we applied similar criteria to events produced in photographic emulsions by 20- and 27-GeV accelerator proton beams. The validity is established in the discussion of Fig. 1, where the low-energy emulsion results are shown.

(6) Our sample of 28.5-GeV pp events has 10^4 interactions of all multiplicities, measured with the Brookhaven National Laboratory flying-spot digitizer (which provides reliable ionization mea-

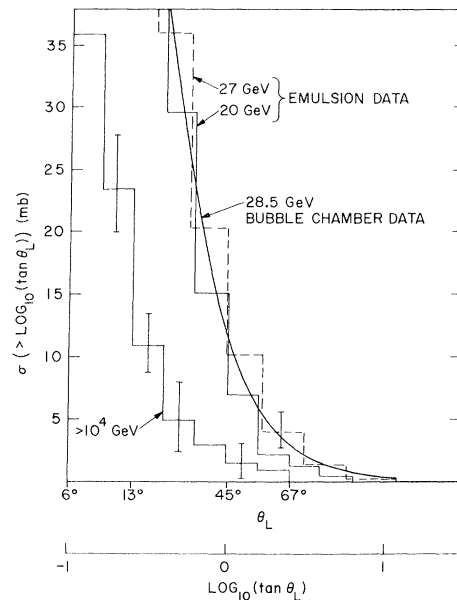


FIG. 1. Integral angular distribution in the large-angle region for accelerator energies 20–30 GeV and cosmic-ray energies above 10^4 GeV.

surement). The plots include all events with four or more prongs. The omission of two-pronged events, which would add at most 6% to the inclusive cross section, does not affect the conclusions drawn. [It is difficult to decide how to include inelastic two-pronged events, because elastic and perhaps quasielastic events, i.e., $p + p \rightarrow p + N^*(I = \frac{1}{2})$, must be excluded.] Two-pronged events broaden the spectra slightly, so that their inclusion would actually strengthen later conclusions.

(7) Our plots are normalized by the requirement that the integral over the entire inclusive spectrum must be the total inclusive cross section, i.e.,

$$\Sigma_I = \int_{U_{\min}}^{U_{\max}} (d\sigma/dU_L) dU_L.$$

The magnitude of $\Sigma_I(28.5)$ is easily computed [Eq. (2)] from the values of \bar{n}_s and σ_{tot} measured in the bubble-chamber data. The same value of σ_{tot} is assumed for computing $\Sigma_I(\geq 10^4)$, an assumption consistent with cosmic-ray data showing total cross sections to be essentially energy-independent.¹³ Thus Σ_I varies as \bar{n}_s . Our estimate of $\Sigma_I(\geq 10^4)$ may be somewhat too large since σ_{tot} for pion primaries is expected to be smaller (by not more than 50%).¹³ As we shall see, the normalization uncertainty does not affect gross comparisons with 28.5-GeV data; the direction of the uncertainty if anything strengthens the

later conclusions. The values are $\Sigma_I(28.5) = 115$ mb and $\Sigma_I(\geq 10^4) = 350$ mb.

(8) Studies of data at < 30 GeV show that the shapes of the target-fragmentation spectra are remarkably independent of the nature of the beam particle³; this leads us to assume that, similarly, at $\geq 10^4$ GeV primary momentum the spectra of pion-produced and nucleon-produced secondaries are shaped alike.

The data, selected according to the foregoing criteria, yield differential inclusive cross sections $d\sigma/dU_L$, plotted as a function of U_L in Fig. 2. The different primary energies are indicated by the arrows for the different mean values \bar{U}_L . The spectra are nearly Gaussian¹⁴ both at 28.5 and at $\geq 10^4$ GeV.

If the inclusive spectra were to scale as predicted by multiperipheral models¹⁵ with ~ 30 GeV as the starting point, at 10^4 GeV the spectrum would appear as indicated by the smooth curve shown in Fig. 2. (The dashed line shows, in an approximate way, how this predicted curve would be modified to include events with primaries $> 10^4$ GeV). The expected plateau is not seen; instead, the cross section at $y_0 = 0$ ($\theta_c \approx 90^\circ$) appears about twice as large at 10^4 as at 30 GeV.

If the inclusive spectra of target fragments reach an energy-independent limit at 28.5 GeV, distributions should overlap at large U_L . If all particles produced backwards in the c.m. system are assumed to be target fragments, then for the backward hemisphere, which corresponds roughly to $U_L > -0.6$ ($\theta_L > 14^\circ$), the spectrum could, in principle, be energy independent. However, for $U_L > -0.06$, the 28.5-GeV data are, bin by bin, consistently higher than the data at $\geq 10^4$ GeV by a factor ≈ 3 . A more stringent test would be for $U_L \geq 0$ which roughly corresponds to lab momenta $\lesssim 0.5$ GeV since $\bar{p}_L \sim 0.3-0.4$ GeV independent of primary energy. Indications of limiting behavior have been seen at primary energies < 30 GeV for pion spectra with < 0.5 GeV in the lab.^{2,3} The selection criterion that $\beta > 0.7$ for plotted tracks [item (3) above] infers that these tracks with $U_L \approx 0$ are mainly pions. It is seen in Fig. 2 that for $U_L > 0$ the compared distributions remain significantly different (more on this below).

The large-angle region is studied in more detail in Fig. 1, in terms of the integrated cross section

$$\sigma(> U_L) \equiv \int_{U_L}^{\infty} (d\sigma/dU_L) dU_L.$$

The smooth curve in Fig. 1 represents the bubble-chamber data.

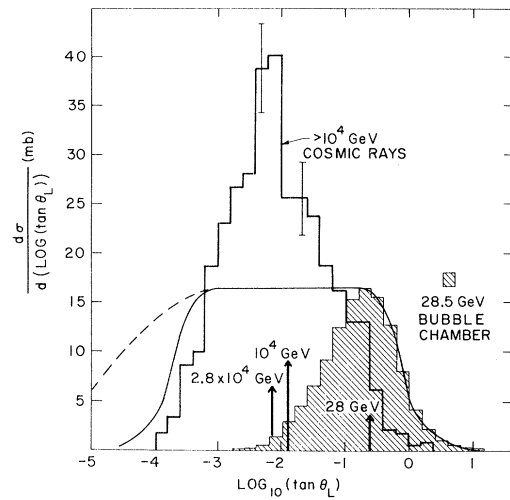


FIG. 2. Differential angular distributions for 28.5-GeV pp interactions and cosmic-ray energies above 10^4 GeV. Central values of rapidity distributions are indicated by arrows for 2.8×10^4 , 10^4 , and 28 GeV. The solid and dashed lines are multiperipheral model predictions discussed in the text.

The aforementioned exposures [item (5)] of emulsions to 20- and 27-GeV proton beams at the CERN proton synchrotron yield the distributions, extracted from publications,¹⁶ shown in Fig. 1. These distributions show excellent agreement with the 28.5-GeV bubble-chamber data. This agreement lends support to the validity of the emulsion technique in selecting hydrogenlike events, and so to the inference that the same selection procedure is valid for the cosmic-ray events at $\geq 10^4$ GeV.

Comparing the 20-, 27-, and 28.5-GeV data with the $\geq 10^4$ -GeV data shows that the lower-energy cross sections are significantly larger for all U_L . For $U_L > 0$ (fragmentation region) it is seen that

$$\frac{d\sigma}{dU_L} (< 30 \text{ GeV}) \approx 3 \frac{d\sigma}{dU_L} (\geq 10^4 \text{ GeV}).$$

Regardless of the justification of identifying pure hydrogen with hydrogenlike interactions, comparison of the emulsion data at < 30 GeV with that at $\geq 10^4$ GeV can be interpreted as fragmentation of the nuclear targets. The conclusion is the same; namely, the inclusive-spectrum cross section changes in the target-fragmentation region, $U_L \geq 0$, approximately as $(\ln s)^{-1}$, where s is the squared c.m. energy.

If the shapes of the plotted spectra are correct, this decrease in cross section seems inescapable. As discussed earlier, the data are normalized

so that the areas of the distributions, Fig. 1, are equal to the respective inclusive cross sections. The value of $\Sigma_I(28.5)$ is probably slightly low [item (6)], while $\Sigma_I(\geq 10^4)$ is probably somewhat large [item (4)], indicating that the observed energy variation, if inaccurate, is larger. Furthermore, if one were to renormalize $\Sigma_I(\geq 10^4)$ so that the spectra would overlap in the large, $U_L \geq 0$, region, the product $\bar{n}_s(\geq 10^4)\sigma_{\text{tot}}(\geq 10^4)$ would have to be increased by a factor ~ 3 , an increase inconsistent with the experimental values of these quantities. Accordingly, the conclusion is maintained that the cross section in the fragmentation region decreases as $\sim (\ln s)^{-1}$ in the range ≤ 30 GeV to $\geq 10^4$ GeV.

We would like to thank R. R. Kinsey, T. W. Morris, and other members of the Brookhaven National Laboratory Bubble Chamber Group who were involved in the analysis of the 28.5-GeV/c $p\bar{p}$ data. One of us (L.v.L.) greatly appreciates the hospitality of the Brookhaven National Laboratory.

*Work supported by the U. S. Atomic Energy Commission.

†Work supported by Bundesministerium für Bildung und Wissenschaft, Bonn, Germany.

‡Work supported by the National Science Foundation.

¹J. Benecke *et al.*, Phys. Rev. **188**, 2159 (1969); R. P. Feynman, in *High Energy Collisions, Third International Conference at Stony Brook, N. Y.*, edited by J. A. Cole *et al.* (Gordon and Breach, New York, 1969), and Phys. Rev. Lett. **23**, 1415 (1969).

²Recent reviews of phenomenology and experiments on this subject include, L. van Hove, Phys. Rep. **1C**, 7 (1971); E. L. Berger, ANL Report No. ANL/HEP 7134, 1971 (unpublished); and W. R. Frazer, in *Phenomenology in Particle Physics, 1971, Proceedings of the Conference at the California Institute of Technology, Pasadena, 25-26 March 1971* (California Institute of Technology, Pasadena, 1971), p. 43.

³M.-S. Chen *et al.*, Phys. Rev. Lett. **26**, 1585 (1971), and references therein.

⁴L. W. Jones *et al.*, Phys. Rev. Lett. **23**, 1671 (1970); D. G. Lyon, ANL Report No. ANL/HEP 7107, 1970 (unpublished).

⁵L. G. Ratner *et al.*, Phys. Rev. Lett. **27**, 68 (1971).

⁶Rapidity is discussed by Feynman, Ref. 1; C. DeTar, Phys. Rev. D **3**, 128 (1971); and also see early reference by A. A. Robb, *Optical Geometry of Motion* (Cambridge U. Press, Cambridge, England, 1911).

⁷J. Gierula and W. Wolter, Acta Phys. Pol. **B2**, 95 (1971).

⁸G. Castagnoli *et al.*, Nuovo Cimento **10**, 1539 (1953); L. von Lindern, Nuovo Cimento **48**, 289 (1967).

⁹A. Barbaro-Galtieri *et al.*, Nuovo Cimento **20**, 487 (1961).

¹⁰A. G. Barkov *et al.*, Phys. Rev. **122**, 617 (1961).

¹¹ICEF (International Co-operation on Emulsion Flights), Nuovo Cimento, Suppl. **1**, 1039 (1963).

¹²Relative scanning efficiencies as a function of multiplicities are discussed by Barkov *et al.*, Ref. 10; and M. Koshiha *et al.*, Nuovo Cimento, Suppl. **1**, 1091 (1963).

¹³See for example, N. A. Dobrotin, in *Proceedings of the Sixth Interamerican Seminar on Cosmic Rays, La Paz, Bolivia, 1970* (Universidad Mayor de San Andrés, La Paz, 1970), and references therein.

¹⁴L. D. Landau, Izv. Akad. Nauk, SSSR **17**, 51 (1953); L. von Lindern, Nuovo Cimento **5**, 491 (1957); see also Ref. 8.

¹⁵Multiperipheral model predictions are discussed by A. Pignotti, ANL Report No. ANL/HEP 7107, 1970 (unpublished); C. de Tar, Ref. 6.

¹⁶H. Goings, Nucl. Phys. **43**, 662 (1963); A. Manz, Nuovo Cimento **44**, 967 (1966). These data are also normalized by Σ_I as discussed in text.